Effect of Stress on the Membrane Capacitance of the Auditory Outer Hair Cell

Kuni H. Iwasa
Laboratory of Cellular Biology, National Institute of Deafness and other Communicative Disorders, National Institutes of Health, Bethesda, Maryland 20892 USA

ABSTRACT The membrane capacitance of the outer hair cell, which has unique membrane potential-dependent motility, was monitored during application of membrane tension. It was found that the membrane capacitance of the cell decreased when stress was applied to the membrane. This result is the opposite of stretching the lipid bilayer in the plasma membrane. It thus indicates the importance of some other capacitance component that decreases on stretching. It has been known that charge movement across the membrane can appear to be a nonlinear capacitance. If membrane stress at the resting potential restricts the movement of the charge associated with force generation, the nonlinear capacitance will decrease. Furthermore, less capacitance reduction by membrane stretching is expected when the membrane is already extended by the (hyperpolarizing) membrane potential. Indeed, it was found that at hyperpolarized potentials, the reduction of the membrane capacitance due to stretching is less. The capacitance change can be described by a two state model of a force-producing unit in which the free energy difference between the contracted and stretched states has both electrical and mechanical components. From the measured change in capacitance, the estimated difference in the membrane area of the unit between the two states is about 2 nm^2.

INTRODUCTION

The motility of the outer hair cell (OHC) from the mammalian cochlea is considered to be essential for fine tuning (1–4). It has been shown that that the fast motility of the OHC is membrane potential-dependent and the amplitude of the movement approaches 2 μm, quite unusual for a nonmuscle cell (5–8). This motility is not ATP-dependent (9). In a previous report (10), it was shown that deformations of the cell due to internal pressure application can be described by a membrane model with an area and a shear modulus. These elastic moduli, combined with the amplitude of the fast motility, indicate that the potential-dependent force is about 0.5 nN/mV for a single OHC. The evaluation of the force enables us to examine energetics of the electromechanical transduction. It is shown that the electrical energy used and the mechanical energy produced by the cell agree within a factor of two or three, indicating a direct conversion of the energy on a molecular level.

In order to obtain a more detailed physical picture of force generation, two questions must be addressed: What is the origin of the elasticity and what is the nature of mechanoelectric coupling? Although the magnitude of the shear modulus relative to the area modulus (about 10%) indicates that cytoskeletal elements are important in the elasticity of the OHC, it is unclear whether the area modulus is attributable to lipid bilayer or cytoskeletal elements. If the lipid bilayer is the main factor in the area modulus, membrane stretching would increase the area of lipid bilayer and reduce the thickness of it. If, on the other hand, the cytoskeleton is the main factor that responds to the stress, the membrane should have considerable folding, and its area would remain unchanged. This can be tested by monitoring the capacitance of the cell during stress application.

Capacitance measurement is also useful in examining mechanoelectrical coupling of the cell. It has been shown that charge movements, such as gating charges of ion channels, contribute to the membrane capacitance. If charge movements are coupled with the fast motility, they should be affected by membrane stress, resulting in a change in the apparent membrane capacitance of the cell.

To address these issues, the membrane capacitance of the OHC was measured during application of membrane stress. The membrane capacitance of the cell was measured with a lock-in amplifier operating between 1 and 2 kHz, and stress was applied either by a direct pressurization of the cell with the recording pipette or by a brief perfusion with a hypoosmotic medium. It was shown that the capacitance decreases when the cell membrane is stretched. This implies that the elasticity of the OHC is mainly attributable to the cytoskeleton and that the movement of force-producing charge is affected by stretching of the membrane.

MATERIALS AND METHODS

Outer hair cells were isolated from guinea pig cochleas by gentle tritulation (in Leibovitz L-15 medium), as reported earlier (11). No digestive enzymes were used for the isolation. Isolated cells were placed in a plastic-bottomed chamber under an inverted microscope (Diavert, Leitz) with 40 × objective for observation. Cells used ranged from 50 to 75 μm in length.

Recording pipettes were made from glass capillaries (blue tip; Oxford, St. Louis, MO) with a two-stage puller (pp 83; Narishige, Tokyo). The resistance of the pipettes used ranged between 1 and 2 MΩ.

For measuring the membrane capacitance, a lock-in amplifier (model 393; Ithaco, Ithaca, NY), operating at a frequency range between 1 and 2

Received for publication 7 December 1992 and in final form 10 February 1993.

Address reprint requests to Kuni H. Iwasa, Laboratory of Collular Biology, NIDCD, National Institutes of Health, Bldg. 10, Rm. 5D46, Bethesda, MD 20892.

0006-3495/93/07/492/07 $2.00

kHz, was used in combination with a patch amplifier (EPC 7; List, Darmstadt, Germany). The amplitude and phase of the current response to a sinusoidal voltage wave (1 mV peak-to-peak) superposed on holding potentials were recorded from a cell in the whole-cell recording configuration during stress application and used for obtaining the membrane capacitance. The patch amplifier was run without capacitance or series resistance compensation, and its output to the lock-in amplifier was not filtered. The time constant setting for the lock-in amplifier was 125 ms.

Two methods were used to apply stress to the entire cell membrane. In one of the methods, a positive pressure was delivered to the cell through the recording pipette in the whole-cell recording configuration. In the other method, membrane stress was applied by brief extracellular perfusion with hypo-osmotic medium. The former has an advantage in that a known pressure could be applied to the cell, but may have a disadvantage of changing the access resistance to the cell in the process. The latter, an osmotic method, does not change the access resistance of the cell. A drawback of this method, however, is that estimating the pressure applied from the length change requires using the calibration plot previously obtained (10). With either method it was difficult to maintain the stress for more than a few seconds without destroying the seal between the cell and the recording pipette. Details of these two methods for applying membrane stress have been reported previously (10, 11).

The standard bath medium consisted of (in millimolar) NaCl 140, KCl 5, $MgCl_2$ 2, $CaCl_2$ 1.5, and 4-(2-hydroxyethyl)-1-piperazineethanesulfonic acid (HEPES) 10. The pipette medium contained (in millimolar) potassium gluconate 145, NaCl 1, $MgCl_2$ 2, EGTA 0.1, $CaCl_2$ 0.058, and HEPES 10. The pH of both media are adjusted to 7.4, and the osmolarity was adjusted to 300 mOsm/kg with glucose. For experiments in which osmotic stress was applied, low ionic-strength external media were used. The medium with the normal osmolarity was obtained by adding nonelectrolyte to low-osmolarity medium. The normal osmolarity medium consisted of (in millimolar) NaCl 90, KCl 5, $MgCl_2$ 2, $CaCl_2$ 1.5, stachiose 100, and HEPES 10, and the low-osmolarity medium did not contain stachiose.

In order to evaluate the capacitance of the cell, an equivalent circuit which consists of membrane resistance R_m, membrane capacitance C_m, and an access resistance R_a was used (Fig. 1). The complex admittance y of the system is given by

$$y = \frac{1 + i\omega C_m R_m}{R_a + R_m + i\omega C_m R_a R_m}, \quad (1)$$

where ω ($= 2\pi f$) is the angular frequency. If we know the absolute value and phase of the complex admittance y for two frequencies ω_1 and ω_2, we can obtain R_m, C_m, and R_a. To determine these values at zero applied pressure, the operating frequency was varied between 1 and 2 kHz. The performance of the setup was tested with a dummy cell with multiple settings. This cell had five settings for C_m between 0 and 60 pF, 20 MΩ, 50 MΩ, and ∞ for R_m, and 0, 1, and 2 MΩ for R_a. To simulate the experimental condition, a series of tests was carried out in which one of the elements in the dummy circuit was switched from one value to another. The outputs of the lock-in amplifier changed on a time scale consistent with the time constant setting. The phase and absolute value outputs from the lock-in amplifier operating at 1, 1.5, and 2 kHz were plotted against theoretical values for these quantities corresponding to the settings. These calibration plots for both the absolute value and the phase were linear, and they were used for determining the phase and absolute value of the complex admittance in the experiment. During stress application the absolute value and phase were monitored, while the lock-in amplifier was operated at one frequency, usually at 1 kHz, because the duration of the stress application is limited to several seconds.

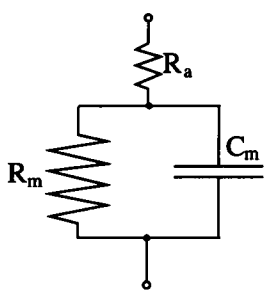

FIGURE 1 Equivalent circuit for evaluating the membrane capacitance. The access resistance R_a corresponds to the pipette resistance in the whole-cell mode. The membrane resistance is represented by R_m and the membrane capacitance by C_m.

RESULTS

First, we determined the membrane capacitance of the cell before application of membrane stress. Examples of the parameters obtained from the complex admittance measured at frequencies 1 and 1.5 kHz are shown (Table 1). The typical membrane capacitance was about 30 pF at −50 mV, near the resting membrane potentials of these cells. The membrane potential dependence of the capacitance is discussed later.

Using these values for the membrane capacitance and membrane and access resistance, it is possible to determine which component changed during application of membrane stress while operating the lock-in amplifier at one frequency. This is necessary because the duration of stress application is rather limited, up to several seconds, to maintain the seal between the cell and pipette for whole-cell recording.

A small increase in the access resistance R_a decreases both the absolute value and the phase of y. A small increase in the membrane resistance R_m increases both the absolute value and the phase of y, but the absolute value is relatively insensitive to the membrane resistance R_m. A small increase in the membrane capacitance C_m increases the absolute value and decreases the phase of y (Fig. 2). Thus a change in the capacitance can be qualitatively distinguished from a change in either of the resistances.

When a positive pressure was applied to the cell through the recording pipette, the absolute value and the phase of the output current underwent complex changes (Fig. 3). The phase φ increased rapidly in the beginning and slowly thereafter during the pressure application. The absolute value A initially increased and then decreased. The response thus had two phases. In the first phase both the phase φ of the complex admittance and the absolute value A increased. The second

TABLE 1 The membrane capacitance C_m, the membrane resistance R_m, and the access resistance R_a

Cell	C_m	R_m	R_a
	pF	MΩ	MΩ
8-Jun 18	36.5 ± 2	12. ± 2	1.4 ± 0.1
3-Jun 18	35.8 ± 3	48. ± 5	3.5 ± 0.4
1-Aug 19	24. ± 3	60. ± 2	5.5 ± 0.3
2-Aug 26	10.5 ± 1	35. ± 5	2.1 ± 0.5
1-Sep 25	34. ± 1	65. ± 6	2.9 ± 0.1

The absolute value and the phase of the complex admittance at 1 and 1.5 kHz were used to determine the membrane capacitance, the membrane resistance, and the access resistance. For two frequencies, Eq. 1 provides four equations (two for real part and one for imaginary part) to determine the three unknown quantities. Thus one equation not used for obtaining these quantities provides an error test. These errors are indicated in the table. The membrane potential was held at −50 mV.

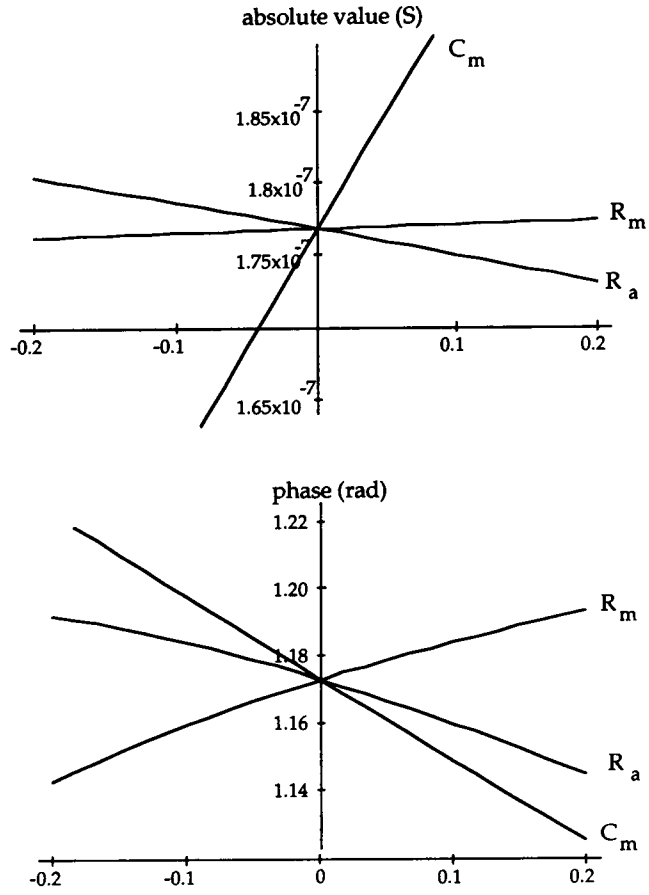

FIGURE 2 Effect of a change in the capacitance C_m and the resistances R_a and R_m on the absolute value A and the phase φ of complex admittance. The abscissa of the plot is the relative changes of these parameters, i.e., either $\Delta C_m/C_m$, $\Delta R_a/R_a$, or $\Delta R_m/R_m$, depending on the label. The reference point chosen is R_a = 1.5 MΩ, R_m = 40 MΩ, C_m = 30 pF. An increase in the access resistance R_a decreases both the phase φ and the absolute value A. An increase in the membrane resistance increases the phase φ but it is ineffective in changing the absolute value A. An increase in the membrane capacitance decreases the phase φ and increases the absolute value A. Thus it is convenient to monitor the phase and the absolute value of the complex admittance during a experiment, because a capacitance change can be recognized as opposite changes in these two observed quantities.

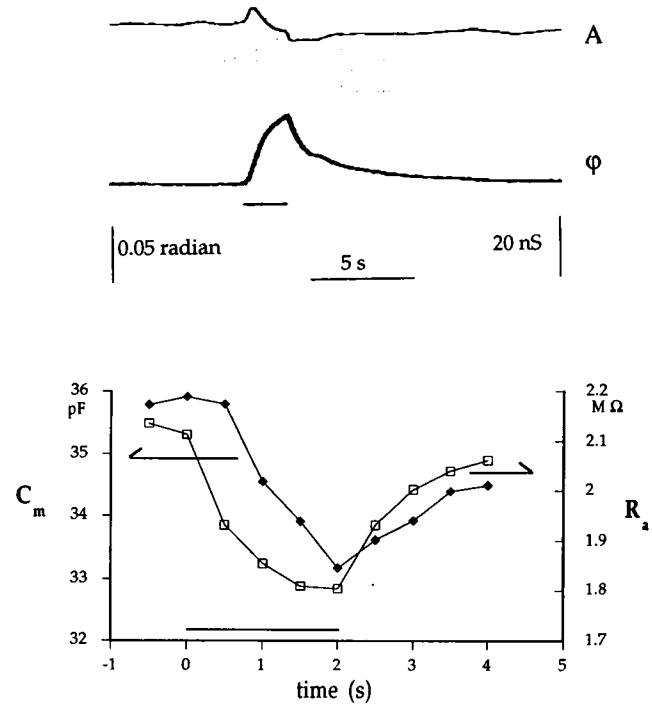

FIGURE 3 Effect of pressure application with the recording pipette. The cell is under voltage clamp in the whole-cell recording configuration. The holding potential is −40 mV. The superposed sinusoidal wave is 1 kHz and 1 mV peak to peak. Top: The phase φ and the absolute value A of the complex admittance. A bar immediately under the traces indicates the time period a positive pressure of 1.2 kPa is delivered to the pipette. An initial increase in the absolute value A is followed by a decrease, while the phase φ was still increasing. Bottom: the membrane capacitance C_m (◆) and the access resistance R_a (□) evaluated assuming that membrane resistance R_m is constant at 20 MΩ. The pipette pressure during the pressure application is 1.2 kPa. A reduction in access resistance precedes an increase in the membrane capacitance.

phase was characterized by a slow increase in the phase φ and decrease in the absolute value A. On the removal of the pressure, both the phase φ and the absolute A value gradually recovered.

The first phase is either a reduction in the access resistance R_a or an increase in the membrane resistance R_m (cf. Fig. 2). The membrane resistance R_m is unlikely to change before the membrane tension is fully developed, and, if it changes, it must decrease due to the presence of stretch-activated channels (11). Thus the change must be attributed to a reduction of the access resistance R_a. Indeed a positive pressure at the pipette must clear the mouth of the pipette of cellular material, and it should result in a reduction in the access resistance R_a. The second phase requires a decrease in the membrane capacitance, because only a capacitance decrease can bring about the observed change (cf. Fig. 2). An analysis (Fig. 3, bottom) shows that the access resistance dominates the first phase of the response and the membrane capacitance is reduced during the pressure application. This interpretation can be confirmed using another method of applying stress to the cell membrane.

Membrane tension can also be applied by perfusing the cell with a hypo-osmotic medium (see Materials and Methods). Unlike the pattern of the responses to pressure application through the pipette, the pattern of the responses to osmotic stress was simple. A decrease of the absolute value A of admittance was accompanied by slight changes in phase φ during the stress (Fig. 4 *a*). These data were analyzed with two different assumptions. In one analysis, the membrane resistance R_m was assumed to be constant. In the other analysis, the access resistance R_a was assumed to be constant. These two methods did not give a significant difference in the values of the membrane capacitance (Fig. 4 *b*). It can be seen that the changes in the absolute value are attributable primarily to the membrane capacitance for osmotic experiments.

In both methods of stress application, it was found that the membrane capacitance decreased. The osmotic method can also be used to determine the membrane capacitance as a

function of the strain in the axial direction of the cell (Fig. 4 *c*). Since this strain is linearly related to the membrane stress (10), the membrane capacitance is expected to be a function of the membrane stress.

The decrease in cell capacitance due to stretching is paradoxical if we regard the cell capacitance to be attributable solely to the lipid bilayer part of the plasma membrane. The cell can be electrically equivalent to a capacitor made of two electrodes (electrolyte solutions) of surface area S sandwiching a material with the dielectric constant ϵ (lipid bilayer). The capacitance is then proportional to $\epsilon S/d$. Stretching a lipid bilayer should increase the surface area S and reduce the membrane thickness d. Either of these changes should result in an increase of the membrane capacitance. Thus we should expect an increase, and not a decrease, in the capacitance. Indeed it has been shown that the capacitance of a small patch of membrane is proportional to its membrane area when tension is applied to a patched membrane in the on-cell configuration (12).

This paradox indicates the presence of a membrane component whose capacitance decreases on stretching of the membrane. This component should more than compensate for the capacitance increase due to stretching the bilayer. It has been known that a charge movement across the membrane appears as a nonlinear capacitance. If membrane stress at the resting potential interferes with the movement of the charge associated with force generation, the total capacitance will be affected.

The existence of mobile membrane charges is illustrated by the potential dependence of the membrane capacitance (Fig. 5). It should be cautioned that this voltage dependence may not entirely be attributable to charge movement, because it is reported that the linear capacitance also decreases on hyperpolarization by 3–5 pF (13). The present result is nonetheless consistent with an earlier report on the nonlinear capacitance (13) in its magnitude (8–18 pF) and in its shape.

If the observed capacitance reduction is mainly due to the nonlinear capacitance, less reduction is expected at more hyperpolarized membrane potentials, where the membrane is alrady stretched. Indeed, at hyperpolarized potentials, the reduction of the membrane capacitance due to stretching is less (Fig. 4 *b*). These observations can be explained by a force-producing (motility) element, presumably a protein, that has both electrical and mechanical components of energy, and that is responsible for the direct mechanoelectrical coupling in the OHC (see Discussion).

DISCUSSION

The magnitude of the capacitance

The value for the capacitance obtained in this report is about 30 pF at −50 mV. This value is in agreement with earlier reports (13, 14). It has been noticed that that the specific capacitance for lipid bilayers and neuronal membranes is universal and is 1 μF/cm^2 (15). The surface area of the cell body of an OHC is between 1.2×10^3 and 2.1×10^3 μm^2, the diameter being 10 μm and the length from 40 to 70 μm. The area of stereocilia would be about 5×10^2 μm^2, assuming that an OHC has 60 stereocilia with diameter 0.5 and 5 μm in length. The specific capacitance of 1 μF/cm^2 leads to a whole-cell capacitance between 17 and 26 pF. In addition, the nonlinear capacitance is about 5 pF at −50 mV. Thus the specific capacitance of 1 μF/cm^2 appears to be valid for OHC membrane.

Due to the presence of nonlinear capacitance, the present experiment cannot give a definitive answer to the question as to whether the area modulus is attributable to the lipid bilayer or the cytoskeleton. It is, however, highly unlikely that the lipid bilayer is stretched more than 4% in area without being broken (16). The maximum axial strain 0.15 produced in the experiment corresponds to an apparent membrane area strain of 0.13. (The apparent area strain $\Delta S/S$ and the axial strain $\Delta L/L$ are related by $\Delta S/S = -6/(\gamma - 3) \times \Delta L/L$, where γ is the ratio of the area modulus to the shear modulus (10). The ratio γ is about 10.) The most likely candidate for explaining the rest, if not all, of the apparent area change is a reduction in the waviness of the membrane. This interpretation implies that the area modulus is attributable to the cytoskeleton.

Quantitative description with a two-state model

The tension-dependent capacitance can be explained by a simple two-state model for the force-generating molecules in the cell. For the sake of simplicity, let us assume that a membrane potential-dependent force-producing unit has two states, extended (represented by a subscript e) and contracted (subscript c). Let the Helmholtz free energy in these two states be F_e and F_c. The free energy difference between the two states can be written as

$$F_e - F_c = -q(V - V_0) - at_m, \qquad (2)$$

where q is the charge transferred across the membrane by the conformational change, V the membrane potential, V_0 a constant, and t_m the membrane tension. The first term represents electrical energy, and the second term represents the elastic energy. When either the membrane is hyperpolarized or stretching force is applied to the membrane, the extended state is favored. Thus a is positive and q is negative. The quantity a has the dimensionality of area and it represents the cross section (area) difference of the force-producing unit in the two states. The functional dependence of the free energy on the membrane tension has been discussed by Sachs and Lecar (17) for stretch activated channels. They showed that this functional dependence in general may be quadratic, but it is linear when the two states have equal mechanical compliances. The same arguments will apply for this motility element. Primarily for the simplicity of the model, a linear relationship was used in Eq. 2. The fraction P_e of the force-generating unit in the extended conformation and the fraction P_c in the contracted state are determined by the free energy difference,

$$P_e/P_c = \exp[-(F_e - F_c)/k_B T], \qquad (3)$$

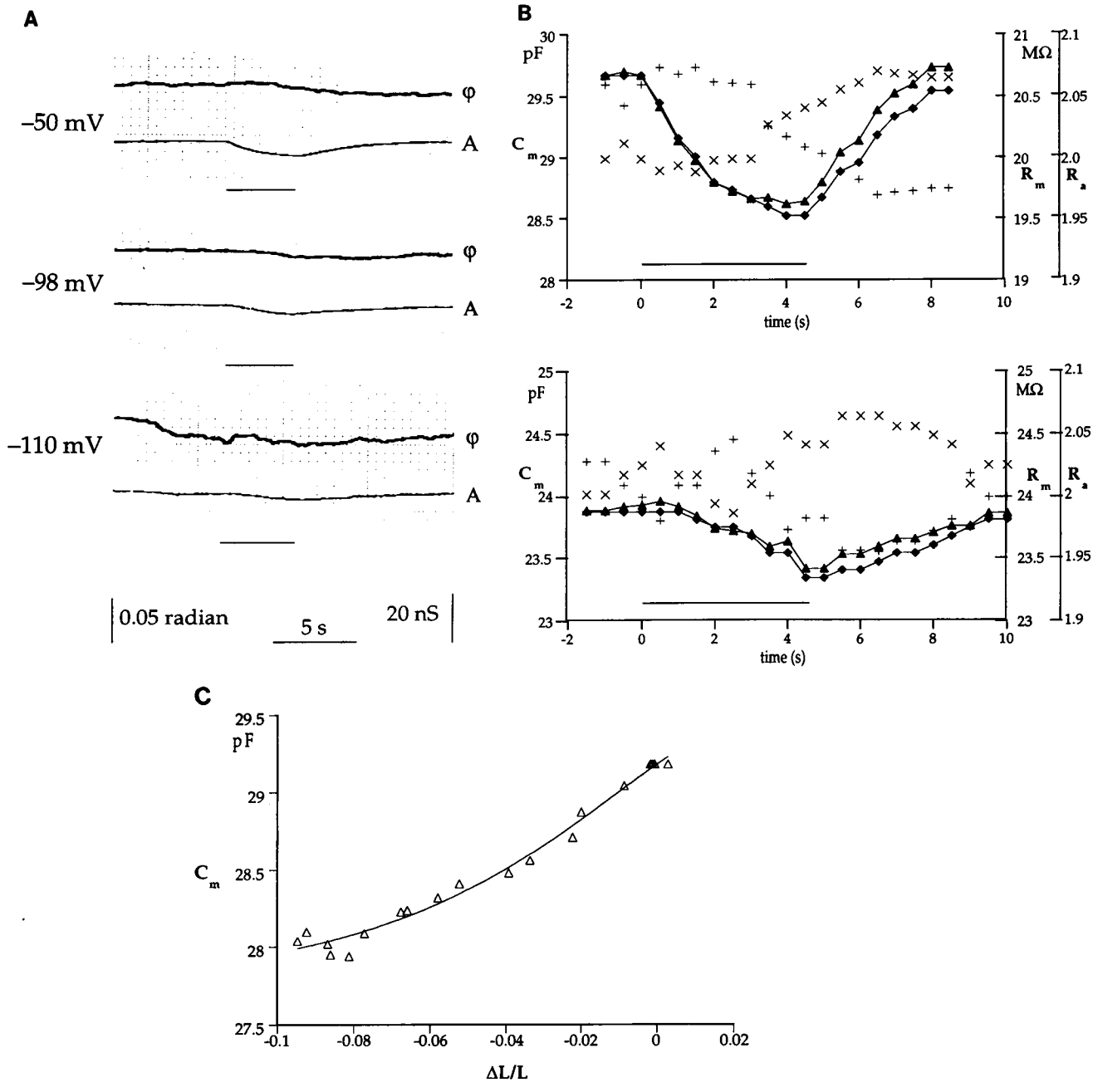

FIGURE 4 Responses to osmotic pressure. The cell is under voltage clamp in the whole cell recording configuration. Hypo-osmotic stress to the cell is applied to the cell by brief perfusion (see Materials and Methods). The resting potential of the cell is −55 mV. (*A*) The phase φ and the absolute value *A* of the complex admittance. The holding potential is indicated on the left. The durations of the hypo-osmotic perfusion are indicated by bars immediately under the traces. The holding potential is indicated. The length change of the cell (60 μm long) due to osmolarity change is about 2.2 μm. (*B*) The membrane capacitance and the resistances at two membrane potentials at −50 mV (*top*) and −110 mV (*bottom*). The data shown in *A* are analyzed based on two alternative assumptions. One is to assume that the access resistance R_a is constant at 2 MΩ (◆ for C_m and × for R_m). This assumption made the membrane resistance larger at more hyperpolarized potential, an expected result. The other assumption is to regard the membrane resistance R_m as constant during osmotic stress (▲ for C_m and + for R_a). R_m is fixed at 20.6 MΩ for 50 mV and 24.3 MΩ for −110 mV. For determination of the membrane capacitance, the choice as to which assumption to make is not important. Horizontal bars indicate duration of hypo-osmotic perfusion. (*C*) The relationship between the membrane capacitance and the membrane strain in the axial direction of the cell. The axial strain and the membrane capacitance of another cell during osmotic stress are plotted. For obtaining the membrane capacitance, the access resistance is assumed to be constant at 2.9 MΩ. The membrane resistance obtained is between 44 and 47 MΩ. An alternative assumption of constant membrane resistance does not make an appreciable difference in the values of the membrane capacitance. The solid curve indicates the best fit with $C_m = C_0 + C_f$, where C_0 is a constant and C_f is given by Eqs. 4 and 5. The linearity of the stress-strain relationship is also assumed. The axial strain 0.07 corresponds to 1-kPa pressure *P* in the cell and the axial tension t_z and the circumferential tension t_c are given by $t_c = rP$ and $t_z = rP/2$, where *r* is the radius of the cylindrical cell (10). Since *r* is about 5 μm and it would be reasonable for the membrane tension t_m to be the average of the tension in two directions, $t_m = (t_c + t_z)/2 = 4.9 \times 10^{-2}\ \Delta L/L$. The fit gives $C_0 = (28 \pm 2)$ pF, $a = (2.1 \pm 0.9)$ nm^2, and $q = (0.6 \pm 0.3)e$, where *e* is the elementary charge. The holding potential is −47.2 mV. The natural length of the cell is 67 μm.

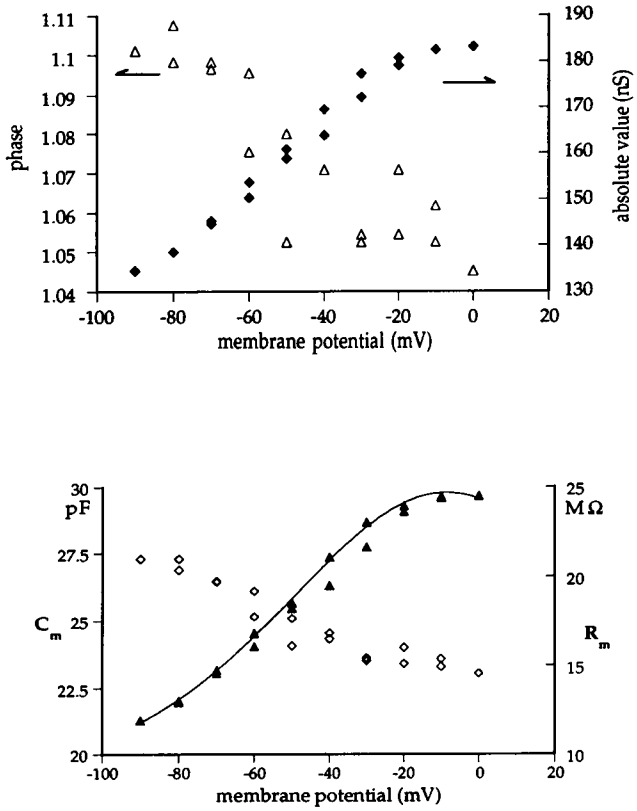

FIGURE 5 Membrane potential-dependence of the membrane capacitance. The plot represents a full cycle of change in the holding potential starting from −100 mV. The membrane capacitance (▲) and the membrane resistance (◇) plotted at the bottom are obtained from the absolute value (◆) and the phase (△) of the complex admittance (plotted at the top) assuming that the access resistance is constant at 2.0 MΩ. The solid curve in the bottom plot indicates the best fit with $C_m = C_0 + C_f$, where C_0 is a constant and C_f is given by Eqs. 4 and 5. The fit gives $C_0 = (18 \pm 1)$ pF and $q = (0.83 \pm 0.1)e$, where e is the elementary charge. The value for q is similar to previously reported values, ranging from 0.5 to 0.8 e (13, 14)

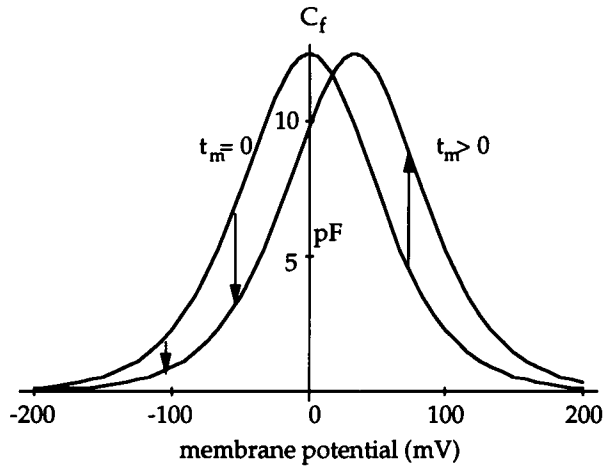

FIGURE 6 Prediction of nonlinear capacitance C_f by a two-state model for potential-dependent force generation. The charge associated with the conformational transition is assumed to be 0.75e, where e is the elementary charge. The reduced mechanical energy at_m/k_BT is assumed to be 1. The number N of the units in the entire cell is assumed to be 5×10^6.

where k_B is the Boltzmann constant, T the temperature, and $P_c + P_e = 1$. The total charge Q_f of the cell attributed to the motile units is then $Q_f = Q_eP_e + Q_cP_c$. Since the difference $Q_e - Q_c$ in the whole cell charge in the two states is based on the charge transfer q of a single motile unit, we have $Q_e - Q_c = Nq$ where N is the number of the motile units in the entire cell membrane. The contribution C_f of the force-generating charge to the capacitance is then $C_f = dQ_f/dV$. Thus we obtain

$$C_f = \frac{Nq^2}{k_BT}\frac{B}{(1+B)^2} \tag{4}$$

with

$$B = \exp\left[-\frac{q(V - V_0) + at_m}{k_BT}\right]. \tag{5}$$

This result predicts that a stress applied to the membrane shifts the peak of the capacitance due to the force-generating charge to more depolarized membrane potential. This is illustrated in Fig. 6. This result can be understood in the following way: The capacitance peak is at the membrane potential corresponding to the steepest transition between the extended and contracted states. Since both membrane tension and hyperpolarized membrane potentials favor the extended state, increased membrane tension elevates the fraction of the extended state for a given membrane potential. Thus an increased membrane tension shifts the peak to a more depolarized potential. This shift explains why the capacitance reduction at a more hyperpolarized potential is less for a given membrane tension (Fig. 6).

Another prediction of this model is that the membrane capacitance of the cell should increase if the membrane potential is clamped to an extremely depolarized level (see Fig. 6). It was difficult to test this prediction, because the membrane quickly became leaky when the membrane potential was clamped to a potential where such an effect is expected.

Equations 4 and 5 allows evaluation of the area difference a of the motile element in the two states. Since the stress-strain relationship in the OHC has been determined (10), strain dependence of the membrane capacitance C_m can be described by Eqs. 4 and 5, assuming that all strain dependence is due to C_f and that the membrane tension t_m is the mean value of the axial tension and the circumferential tension. The strain-capacitance plot can be fit with Eqs. 4 and 5, using this assumption (Fig. 4 c). The fit indicates that the area change a is about 2.1 nm^2. A cruder estimation can be done by comparing Fig. 4 b with Fig. 5. The comparison indicates that a strain of 0.04 (= 2.2 μm/60 μm) produces capacitance reduction equivalent to a shift of about 20 mV in the membrane potential. Equating the electrical energy due to a 20-mV change with the mechanical energy due to the strain of 0.04 gives a similar value for the area change a.

The estimates above assume that none of the capacitance change is caused by the lipid bilayer. If the lipid bilayer stretches up to 4% during membrane tension increasing the linear capacitance, the nonlinear capacitance must decrease

even more to compensate for this increase. This assumption leads to a 50% larger value for a.

The significance of the area change of the motile unit evaluated above may also be examined by relating it to morphological studies. Electron microscopy shows that the lateral membrane of the outer hair cell is packed with particles, presumably protein molecules, with 10-nm diameter (18, 19). These particles are considered to be responsible for the motile response (19), because a similar structure has not been observed in other cells. This individual particle may be the unit in which the area change of 2.1 nm^2 evaluated in this study takes place. Alternatively this area change can be attributed to each subunit which forms these particles. When these change their cross section in the membrane, the linear capacitance should increase. This effect, however, may not be significant, because membrane proteins are usually thicker than lipid bilayers and thus should contribute less to the membrane capacitance than lipid bilayers do.

It is not clear how the tension applied to the cell membrane is conveyed to the motile element without significantly affecting the lipid bilayer component of the membrane. A similar, if not the same, path of transmission in the reverse direction is expected for the membrane potential-dependent force generation. One of the possibilities is that this motile element has direct links with the cytoskeleton and that cytoskeletal links convey tension. Morphological studies show that the cytoskeletal spacing is greater than the spacing of the putative motile elements (19, 20), and thus this interpretation is not supported. An alternative explanation is that the elastic constant of the motile element is smaller than that of lipid bilayers, and lipid bilayers are important for transmitting force between the cytoskeleton and the motile element. Indeed, recent values (1.5–10 N/m) for the area modulus of lipid bilayers (16) are larger than the area modulus (0.07 N/m) of the OHC (10).

While the two-state model probably gives the simplest description of the system, other models can describe the observations equally well. These alternatives include multistate and continuum models. In these models, stress may change the shape of the voltage dependence of the capacitance, whereas in the two-state model the change is limited to a shift in the transition point preserving the shape of the functional dependence. The clarification of such details requires separation of linear and nonlinear capacitance while maintaining a constant membrane stress. It is expected nonetheless that the essential features of the electromechanical coupling are represented by the two-state model.

I thank Dr. Gerald Ehrenstein for valuable comments.

REFERENCES

1. Gold, T. 1948. Hearing II. The physical basis of the action of the cochlea. *Proc. Roy. Soc.* B135:492–498.
2. Davis, H. 1983. An active process in cochlear mechanics. *Hearing Res.* 9:79–90.
3. Brownell, W., C. Bader, D. Bertrand, and Y. Ribaupierre. 1985. Evoked mechanical responses of isolated outer hair cells. *Science.* 227:194–196.
4. Mountain, D. C., and A. E. Hubbard. 1989. Rapid force production in the cochlea. *Hearing Res.* 42:195–202.
5. Ashmore, J. F. 1987. A fast motile response in guinea-pig outer hair cells: the molecular basis of the cochlear amplifier. *J. Physiol. (Lond.).* 388:323–347.
6. Santos-Sacchi, J., and J. P. Dilger. 1988. Whole cell currents and mechanical responses of isolated outer hair cells. *Hearing Res.* 35:143–150.
7. Iwasa, K., and B. Kachar. 1989. Fast in vitro movement of outer hair cells in an external electric field: effect of digitonin, a membrane permeabilzing agent. *Hearing Res.* 40:247–254.
8. Dallos, P., B. N. Evans, and R. Hallworth. 1991. Nature of the motor element in electrokinetic shape changes of cochlear outer hair cells. *Nature.* 350:155–157.
9. Kachar, B., W. E. Brownell, R. Altschuler, and J. Fex. 1986. Electrokinetic shape changes of cochlear outer hair cells. *Nature.* 322:365–367.
10. Iwasa, K. H., and R. S. Chadwick. 1992. Elasticity and active force generation of cochlear outer hair cells. *J. Acoust. Soc. Am.* 92:3169–3173.
11. Iwasa, K. H., M. Li, M. Jia, and B. Kachar. 1991. Stretch sensitivity of the lateral wall of the auditory outer hair cell from the guinea pig. *Neurosci. Lett.* 133:171–174.
12. Sokabe, M., F. Sachs, and Z. Jing. 1991. Quantitative video microscopy of patch clamped membranes stress, strain, capacitance, and stretch channel activation. *Biophys. J.* 59:722–728.
13. Santos-Sacchi, J. 1991. Reversible inhibition of voltage-dependent outer hair cell motility and capacitance. *J. Neurosci.* 11:3096–3110
14. Ashmore, J. F. 1990. Forward and reverse transduction in the mammalian cochlea. *Neurosci. Res. Suppl.* 12:S39-S50.
15. Cole, K. S. 1968. Membrane, ions and impulses, University of California Press, Berkeley, CA. 569 pp.
16. Bloom, M., E. Evans, and O. G. Mouritsen. 1991. Physical properties of the fluid lipid-bilayer component of cell membranes: a perspective. *Quart. Rev. Biophys.* 24:293–397.
17. Sachs, F., and H. Lecar. 1991. Stochastic models for mechanical transduction. *Biophys. J.* 59:1143–1145.
18. Gulley, R. L., and Reese, T. S. 1977. Regional specialization of the hair cell plasmalemma in the organ of Corti. *Anat. Rec.* 189:109–124.
19. Kalinec, E., M. C. Holley, K. H. Iwasa, D. J. Lim, and B. Kachar. 1992. A membrane-based force generation mechanism in auditory sensory cells. *Proc. Natl. Acad. Sci. USA.* 89:8671–8675.
20. Holley, M. C., and J. F. Ashmore. 1990. Spectrin, actin and the structure of the cortical lattice in mammalian cochlear outer hair cells. *J. Cell Sci.* 96:283–291.